PAPER

# Positronium emission from GaN(0001) and AlN(0001) surfaces



IOP Publishing Journal of Physics B: Atomic, Molecular and Optical Physics
J. Phys. B: At. Mol. Opt. Phys. **54** (2021) 205202 (6pp) https://doi.org/10.1088/1361-6455/ac32a0

# Positronium emission from GaN(0001) and AlN(0001) surfaces

**A Kawasuso[1,*], M Maekawa[1], A Miyashita[1], K Wada[2], Y Nagashima[3] and A Ishida[4]**

[1] National Institutes for Quantum and Radiological Science and Technology, 1233 Watanuki, Takasaki, Gunma 370-1292, Japan
[2] High Energy Accelerator Research Organization, 1-1 Oho, Tsukuba, Ibaraki, 305-0801, Japan
[3] Tokyo University of Science, 1-3, Kagurazaka, Shinjuku-ku, Tokyo 162-8601, Japan
[4] The University of Tokyo, 7-3-1, Hongo, Bunkyo-ku, Tokyo 113-0033, Japan

E-mail: kawasuso.atsuo@qst.go.jp

Received 7 August 2021, revised 12 October 2021
Accepted for publication 22 October 2021
Published 23 November 2021

**Abstract**

Positronium emission from wurtzite GaN(0001) and AlN(0001) surfaces was observed by positronium time-of-flight spectroscopy. The positronium energy spectra contained two positronium components distinguished by their energies. Through detailed analyses based on Monte Carlo simulations, these two components were attributed to positronium formed from valence and conduction electrons. The obtained results augment the previous arguments regarding the contribution of conduction electrons to positronium emission from 4H SiC(0001) and Si(111) surfaces.

Keywords: positroniums, emissions, GaN, AlN

(Some figures may appear in colour only in the online journal)

## 1. Introduction

Positronium, the bound state of an electron and a positron [1, 2], has been extensively investigated in fundamental physics [3–5]. Recently, some new challenges, such as positronium Bose–Einstein condensation [6] and the development of positronium beams [7], are steadily being explored. In material physics, positronium spectroscopy plays an important role in probing spin-polarized surface electronic states [8–10]. In these areas, the formation of high-density positronium is a key technology and obtaining a comprehensive understanding of the positronium emission process from solid surfaces is of fundamental importance.

Through extensive studies on positronium emission from metal surfaces, three emission processes have been identified: (i) direct emission from the surface with a negative formation potential, (ii) combination between positrons confined in the surface mirror potential and surface electrons, and (iii) dynamical neutralization of energetic positrons during scattering at the surface [11–14]. In some insulators, positronium Bloch states like Wannier–Mott-type exciton are known to be formed [15]. Such bulk positronium is also thought to be directly emitted into vacuum when the positronium work function is negative [16, 17]. As for semiconductors, several intriguing features, such as almost 100% positronium emission from Ge at high temperatures [11] and optical-excitation-assisted positronium emission from Si [18], have been reported.

From the viewpoint of electrical properties, semiconductors are intermediate materials between metals and insulators. That is, a semiconductor has a finite band gap, but its width is considerably smaller than that of an insulator. In addition, the dielectric constants of semiconductors lie between those of metals and insulators. Therefore, the thermal or optical excitation of electrons from the valence band to the conduction band occurs much more easily for semiconductors than for insulators. The positronium binding energy in the bulk is expected to be small but finite (of the order of 10–100 meV), and hence bulk positronium emission cannot be dismissed in principle. Positronium emission from positrons in the surface mirror potential and surface dangling-bond states is also possible similar to metals.

* Author to whom any correspondence should be addressed.

 

To date, positronium emission from Ge, Si, and 4H SiC surfaces has been investigated [19–22]. In contrast to the sharp rise in the energy spectrum at the negative of the positronium formation potential ($-\Phi_{Ps}$) observed for metals, the energy spectra of semiconductors exhibit high-energy tails above $-\Phi_{Ps}$, implying the contribution of electrons in the excited states to the positronium emission [22]. In this work, we further investigated the positronium emission from GaN(0001) and AlN(0001) surfaces using positronium time-of-flight (PsTOF) spectroscopy. The high-energy positronium components were also observed here.

## 2. Experiment

The GaN(0001) and AlN(0001) samples were undoped wurtzite films of 2 $\mu$m thickness that had been grown by metalorganic chemical vapor deposition on $Al_2O_3$(0001) and purchased from POWDEC K.K. After surface cleaning with ethanol, the samples were transferred into a vacuum chamber. The PsTOF measurements were conducted at the Slow Positron Facility of the High Energy Acceleration Research Organization in Tsukuba, Japan [23, 24]. The sample surfaces were irradiated with a positron beam with an energy of $E_+ = 3$ keV through an aperture of 12 mm diameter located 10 mm upstream of the sample. The average and maximum open angles of detectable positronium were 31° and 50°, respectively, to the surface normal. Annihilation gamma rays from the emitted positronium were detected by two scintillation detectors through slits with widths of $d = 2.2$ and 9 mm at horizontal lengths from the sample of $L = 40$ and 122 mm, respectively. The slit length ($D$) and beam pipe radius ($R$) were 100 and 125 mm, respectively. The above effective horizontal lengths were then $L_{\rm eff} = L - d(1/2 + R/D) = 37$ and 106 mm, respectively. The time to energy conversion was determined with these effective lengths. The time resolution of the electronic system was approximately 10 ns in the full width of the prompt peak. The resolution function was approximated by a Gaussian function with the width of 1/10 of the maximum between the earliest and latest detection times of positronium at the slit ($t_{e,l} = [L \mp d(1/2 + R/D)]/\sqrt{E_{Ps}/m} \mp 5$ ns, where $E_{Ps}$ is the positronium kinetic energy and $m$ is the electron rest mass) and a factor of $t^2 \exp(t/142\ \text{ns})$ for mono-energetic positronium ejected perpendicularly from the surface. Then, by converting the time scale to the energy scale, the energy resolution was obtained. A typical energy resolution was ~1 eV for $E_{Ps} = 3$ eV and it became better (worse) with decreasing (increasing) $E_{Ps}$. This analytical estimation was further confirmed by a Monte Carlo simulation assuming the above geometrical conditions.

## 3. Theoretical calculation

The positron work functions, positronium formation potentials, and related physical quantities were obtained from density functional theory (DFT) calculations using the ABINIT package [25] with the projector augmented-wave method [26] within the generalized gradient approximation (GGA) [27]. The electron–positron correlation energy functional was based on the GGA method [28]. The positronium formation potential was determined as $\Phi_{Ps} = -A_+ - 6.8$ eV, where $A_+$ is the positron affinity, using the primitive cell with full structural optimization and $k$-point sampling of 12 × 12 × 8. The positron work function was determined by $\phi_+ = -A_+ - \phi_-$, where $\phi_-$ is the electron work function calculated for a slab crystal of six bilayers in the surface normal direction with the primitive cell in the surface parallel direction, with $k$-point sampling of 12 × 12 × 1. The (0001) surface was bulk truncated, and the $(000\bar{1})$ surface was terminated with H atoms. The initial vacuum layer was 30 Å. For positrons, only the Γ point was considered. The positron surface state was also calculated with a corrugated mirror potential implemented as the surface potential for positrons [29–32]. The valence electron configurations were $3d^{10}4s^24p^1$ (Ga), $3s^23p^1$ (Al), and $2s^22p^3$ (N). Table 1 lists the calculation results. For both GaN(0001) and AlN(0001), the positron work functions and positronium formation potentials are negative, suggesting spontaneous positron and positronium emission. The positron surface states are also formed. The positron work function for GaN is in agreement with previously determined experimental values [33, 34].

**Table 1.** Calculated positron affinity ($A_+$), positronium formation potential ($\Phi_{Ps}$), electron and positron work functions ($\phi_-$, $\phi_+$), surface dipole barrier ($\Delta_{SD}$) and surface positron binding energy ($E_B$) for GaN(0001) and AlN(0001) surfaces in eV.

| | Bulk calculation | | Slab calculation | | | |
|---|---|---|---|---|---|---|
| | $A_+$ | $\Phi_{Ps}$ | $\phi_-$ | $\phi_+$ | $\Delta_{SD}$ | $E_B$ |
| GaN(0001) | −4.74 | −2.06 | +6.55 | −1.80 | +11.99 | +2.45 |
| AlN(0001) | −4.12 | −2.68 | +7.97 | −3.84 | +15.00 | +3.08 |

## 4. Results

Figures 1(a)–(f) show the positronium energy spectra obtained for the GaN sample. The measurement was conducted first in the as-prepared state (300 K) and subsequently at 1000 and 423 K. The spectra obtained at the two slit positions (40 and 122 mm) were similar to each other. This means that only fast positronium was properly detected in the measurements. In the as-prepared state, the spectrum intensities were rather low. In contrast, upon heating at 1000 K, the intensities increased considerably. This implies that the surface adsorbates in the as-prepared state prevented the positronium emission, whereas the surface became cleaner at 1000 K and positronium emission was facilitated. At 423 K, the intensities were almost maintained. (The intensities were normalized to each prompt peak intensity in the PsTOF spectra.) Thus, the influence of temperature on the positronium energy spectrum was weak. In all of the spectra, in addition to the main parts of the spectra below $-\Phi_{Ps}^{calc}$, high-energy tails were observed to the end points of 6–7 eV. This indicates the existence of two positronium components distinguished by their threshold energies at approximately $-\Phi_{Ps}^{calc}$ and 6–7 eV.

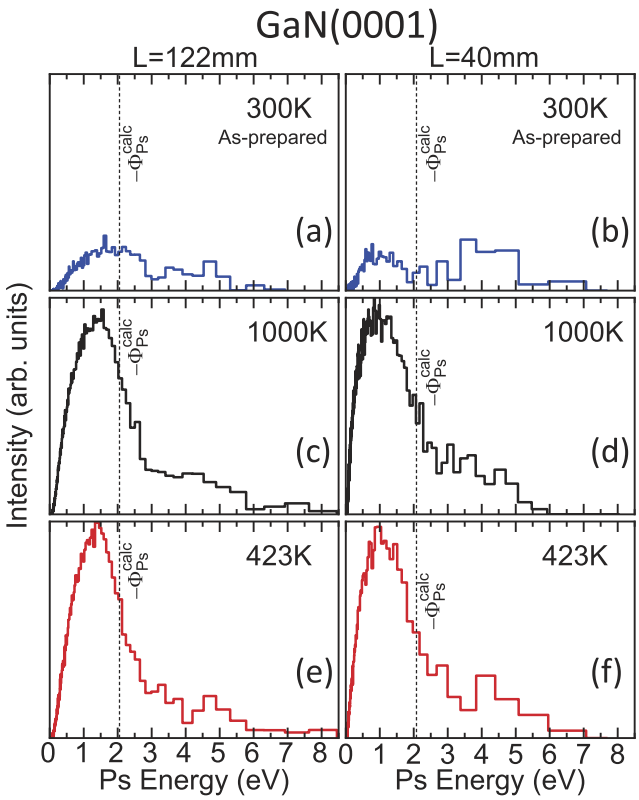


**Figure 1.** Positronium energy spectra obtained for the GaN(0001) sample in the as-prepared state ((a) and (b)), and at 1000 K ((c) and (d)) and 423 K ((e) and (f)) by converting the time scale to the energy scale of the PsTOF spectra at the slit positions of 40 mm (right, (b), (d) and (f)) and 122 mm (left, (a), (c) and (e)). The vertical axes are normalized to the prompt peak intensity such that and hence the individual intensities are mutually comparable.

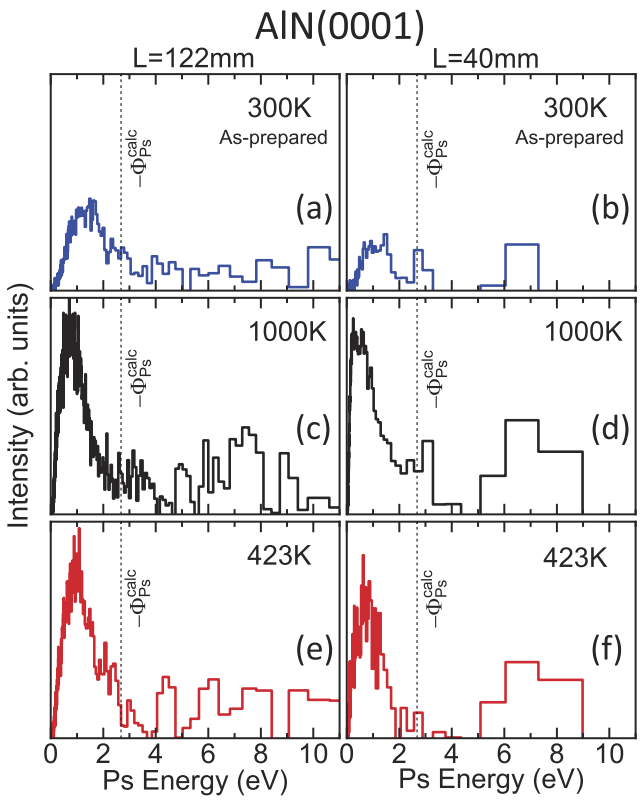


**Figure 2.** Positronium energy spectra obtained for the AlN(0001) sample in the as-prepared state ((a) and (b)), and at 1000 K ((c) and (d)) and 423 K ((e) and (f)) by converting the time scale to the energy scale of the PsTOF spectra at the slit positions of 40 mm (right, (b), (d) and (f)) and 122 mm (left, (a), (c) and (e)). The vertical axes are normalized to the prompt peak intensity such that the and hence individual intensities are mutually comparable.

Figures 2(a)–(f) show the positronium energy spectra obtained for the AlN sample. The measurement sequence was the same as for the GaN sample. Once again, the intensities were rather weak for the as-prepared state but increased after heating, suggesting the surface-cleaning effect upon heating. All of the spectra appeared to contain two positronium components; the main parts of the spectra appeared below $-\Phi_{Ps}^{calc}$ and the high-energy parts emerged at threshold energies of 8–9 eV. These features are basically similar to the results obtained for the GaN sample, except for the values of the threshold energies.

## 5. Discussion

The present results demonstrate positronium emission from the GaN(0001) and AlN(0001) samples, as expected from the negative formation potentials obtained from the DFT calculations. In these calculations, valence electrons were assumed to be the source of positronium. Hence, the main parts of the positronium energy spectra in figures 1 and 2, which rise at approximately $-\Phi_{Ps}^{calc}$, can be attributed to the combination between positrons and valence electrons. The threshold energies of the additional positronium component observed for the GaN and AlN samples were higher than $-\Phi_{Ps}^{calc}$ by 3–4 and 6–7 eV, respectively. These energy separations are close to the band gap energies of 3.4 eV (GaN) and 6.5 eV (AlN). Therefore, the high-energy component observed for both samples may be ascribed to the combination between positrons and electrons located in the in-gap states and the conduction band. In the previous studies of 4H SiC(0001) and Si(111), high-energy thresholds above $-\Phi_{Ps}^{calc}$ with separations similar to the band gap energies were also observed [22]. The positronium energy spectra were also found to be independent of the surface orientation and conduction type. These results imply the importance of conduction electrons as a source of positronium, although surface state electrons may also contribute to the positronium emission.

Figure 3 summarizes the data for GaN(0001) and AlN(0001) together with 4H SiC(0001) and Si(111). (All data were obtained at $L = 122$ mm. In the cases of GaN and AlN, the spectra at 423 K and 1000 K were summed for better statistics.) It can be seen that the two positronium components are clearly separated for the GaN and AlN samples, whereas this separation is somewhat ambiguous for Si and SiC. The wider band gap energies of GaN and AlN presumably give rise to clearer separation of the two positronium components caused by the valence and conduction electrons. However, if that is the case, two positronium components may be clearly separated in SiC, too, because of the wide band gap (~3.2 eV). In this regards, the emission angle of positronium

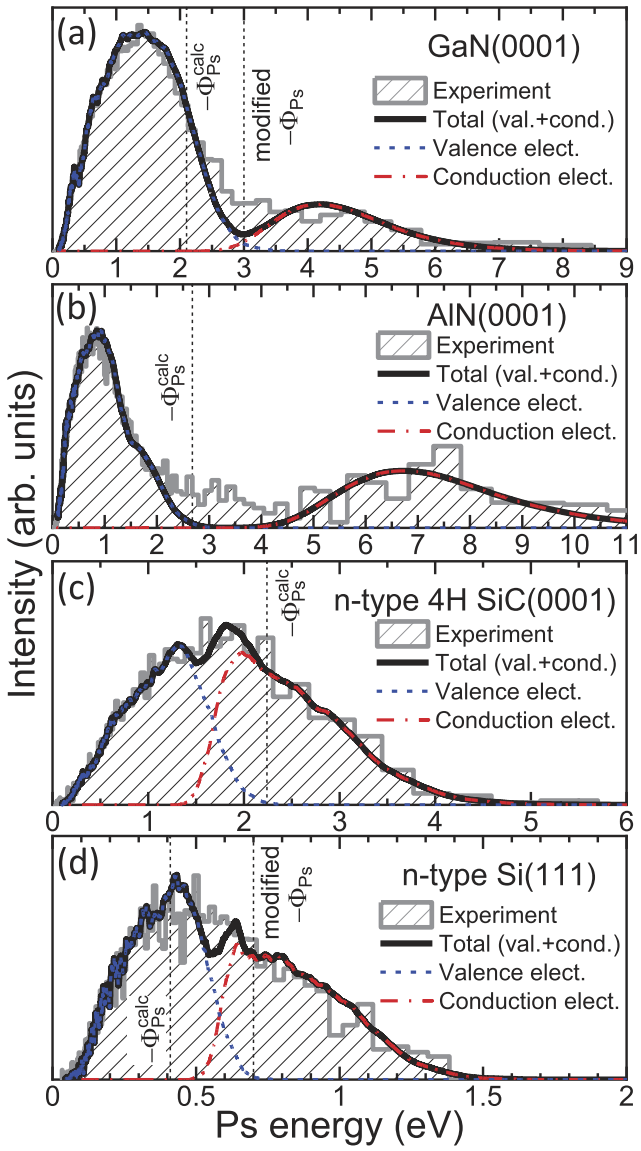


**Figure 3.** Comparison between the experimental energy spectra at $L = 122$ mm and simulated spectra based on the Monte Carlo method for (a) GaN(0001), (b) AlN(0001), (c) SiC(0001), and (d) Si(111) surfaces. For GaN and AlN, the experimental data at 1000 and 423 K were summed to improve the statistics. The gray and black lines represent the experimental and simulated spectra, respectively. The broken and dashed lines show the contributions from the valence and conduction electrons, respectively.

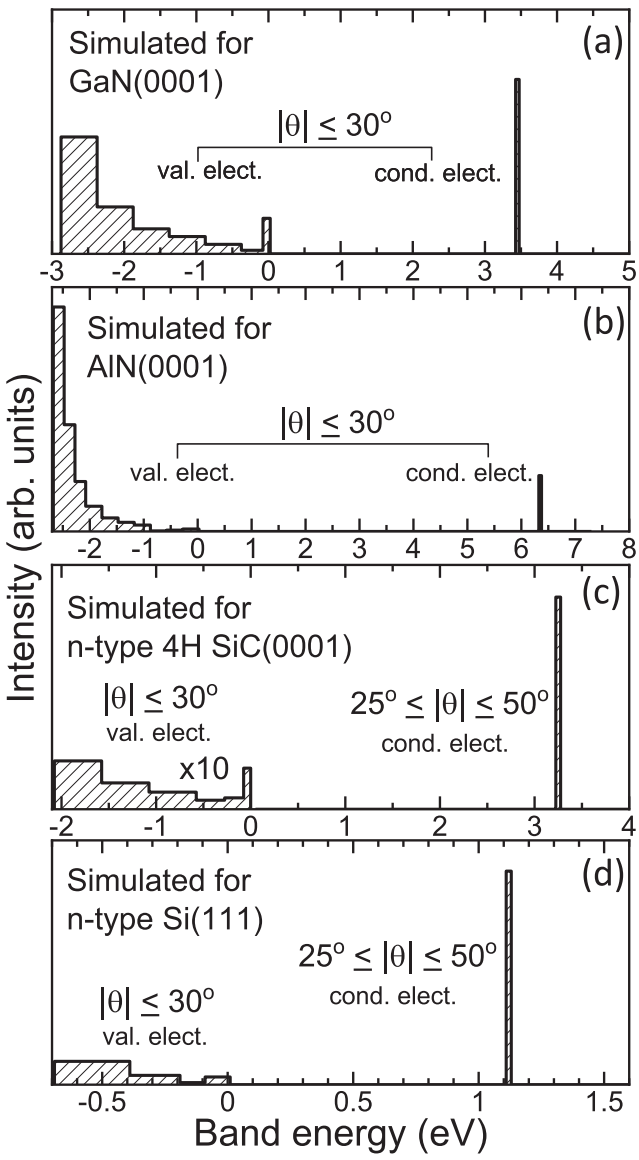


**Figure 4.** Relative intensities of the valence and conduction electrons participating in the positronium formation assumed in the Monte Carlo simulation shown in figures 3(a)–(d). The energy of 0 eV corresponds to the top of the valence band, while the energy position of the sharp peak corresponds to the bottom of the conduction band. The assumed angle widths of emitted positronium are denoted $\theta$.

should also be considered. Because the bottom of the conduction band is located at the Γ point in GaN and AlN owing to their direct band gaps, positronium is ideally emitted in the surface normal direction. In contrast, the bottom of the conduction band is located at the $M$ point in 4H SiC and near the $X$ point in Si, and thus the positronium emission angle should be somewhat deviated from the surface normal direction. The positronium emission angle may be simply estimated as $\tan\theta = k_{\parallel}^{-} / \sqrt{4mE_{Ps}/\hbar^2 - (k_{\parallel}^{-})^2}$, where $k_{\parallel}^{-}$ is the electron wave number parallel to the surface ($k_{\parallel}^{-} = 1.18$ and $0.8$ Å$^{-1}$ for the bottoms of the conduction bands of 4H SiC and Si, respectively, with respect to their surface orientations). Assuming that $E_{Ps} = 5.3$ eV for 4H SiC and 1.8 eV for Si, the emission angle is $\theta = 45°$ for 4H SiC and 56° for Si. Furthermore, the difference in the carrier recombination lifetimes between direct and indirect gap semiconductors should also be considered. The carrier recombination lifetime is basically longer in indirect gap semiconductors [35]. Hence, the conduction electrons in indirect gap semiconductors may have more chances to participate in the positronium formation giving rise to a relatively higher intensity in the energy spectrum. Thus, the above two factors account for the unclearer separation of the two positronium components in the 4H SiC and Si samples than in the GaN and AlN samples.

To confirm the above arguments quantitatively, we performed Monte Carlo simulations of the positronium energy

spectra assuming both valence and conduction electrons as the source of positronium under the actual experimental geometry and system time resolution. To mimic the experimental spectra, the relative intensities of the valence and conduction electrons and the positronium emission angles were varied as the fitting parameters. The positronium formation potentials were first fixed to the values of $\Phi_{Ps}^{calc}$ obtained from the DFT calculations. However, the experimental spectra for Si(111) and GaN(0001) were hardly reproduced with $\Phi_{Ps}^{calc} = -0.4$ eV (Si) and $-2.06$ eV (GaN), and hence these were modified to $-0.7$ and $-3.0$ eV, respectively. The solid lines in figure 3 represent the simulated positronium spectra. The broken and dashed lines show the contributions from the valence and conduction electrons, respectively. The experimental spectra were well reproduced by the above simulations.

Figure 4 presents the relative intensities of the valence and conduction electrons and the positronium emission angles obtained through the fitting procedure. For the valence bands, electrons located at $E = 0{-}\Phi_{Ps}^{calc}$ were assumed to be picked up by positrons. Although the top of the valence band is located at the $\Gamma$ point, imposing the finite angle distribution of positronium ($|\theta| \leqslant 30^\circ$) formed from the valence electrons afforded better fitting results. Such a finite angle distribution is likely attributable to the phonon effect since the phonon state number normally has a wide distribution in the Brillouin zone. In all the four semiconductors, the intensity of the valence electrons tends to increase with the depth of band energy. This probably reflects the fact that the state number of the valence band increases with the depth of band energy. As discussed in the preceding paragraph, the emission angle of positronium formed from conduction electrons is ideally 0° for GaN and AlN, 45° for 4H SiC, and 56° for Si. To reproduce the experimental spectra, finite angle distributions, i.e., $|\theta| \leqslant 30^\circ$ for GaN and AlN and $25^\circ \leqslant |\theta| \leqslant 50^\circ$ for 4H SiC and Si, were again required. In fact, in the case of Si, without the angle distribution, the positronium cannot pass through the aperture because the above emission angle is outside of the maximum acceptance (50°). As expected from the arguments related to the carrier recombination lifetime, the intensity of the conduction electrons is larger in Si and SiC than in GaN and AlN.

## 6. Conclusion

Positronium formation at GaN(0001) and AlN(0001) surfaces was investigated by PsTOF spectroscopy and DFT calculations. For both surfaces, two positronium components distinguished by their threshold energies were identified. These were attributed to positronium formed from valence and conduction electrons. The obtained positronium energy spectra were compared with those for the 4H SiC(0001) and Si(111) surfaces reported previously. The difference between the direct-gap semiconductors (GaN and AlN) and the indirect-gap semiconductors (4H SiC and Si) can be explained by the difference in the emission angles of positronium formed from conduction electrons and also by the difference in the carrier recombination lifetimes.

## Acknowledgments

This work was partially supported by JSPS KAKENHI under Grants No. 20K05454.

## Data availability statement

All data that support the findings of this study are included within the article (and any supplementary files).

## ORCID iDs

A Kawasuso https://orcid.org/0000-0002-7065-5753
M Maekawa https://orcid.org/0000-0001-9172-1206
A Miyashita https://orcid.org/0000-0002-2829-1941
K Wada https://orcid.org/0000-0002-8694-1332
Y Nagashima https://orcid.org/0000-0003-1521-1815
A Ishida https://orcid.org/0000-0002-9880-6517

## References

[1] Mohorovičić S 1934 *Astron. Notes* **253** 94
[2] Deutsch M 1951 *Phys. Rev.* **82** 455
[3] Rubbia A 2004 *Int. J. Mod. Phys.* A **19** 3691
[4] Karshenboim S G 2005 *Phys. Rep.* **422** 1
[5] Cassidy D B 2018 *Eur. Phys. J.* D **53** 72
[6] Shu K *et al* 2017 *J. Phys.: Conf. Ser.* **791** 012007
[7] Michishio K, Chiari L, Tanaka F, Oshima N and Nagashima Y 2019 *Rev. Sci. Instrum.* **90** 023305
[8] Miyashita A, Maekawa M, Wada K, Kawasuso A, Watanabe T, Entani S and Sakai S 2018 *Phys. Rev.* B **97** 195405
[9] Miyashita A, Li S, Sakai S, Maekawa M and Kawasuso A 2020 *Phys. Rev.* B **102** 045425
[10] Maekawa M, Miyashita A, Sakai S, Li S, Entani S, Kawasuso A and Sakuraba Y 2021 *Phys. Rev. Lett.* **126** 186401
[11] Mills A P 1978 *Phys. Rev. Lett.* **41** 1828
[12] Mills A P 1979 *Solid State Commun.* **31** 623
[13] Mills A P 1993 *Positron Spectroscopy of Solids* ed A Dupasquire and A P Mills (Ohmsha, Amsterdam, Oxford, Tokyo, Washington DC: IOS Press) p 209
[14] Ishii A 1992 *Sol. Stat. Phen.* **28–29** 213
[15] Dupasquier A 1983 *Positron Solid-State Physics* ed W Brandt and A Dupasquier (Amsterdam: North-Holland) p 510
[16] Schultz P J and Lynn K G 1988 *Rev. Mod. Phys.* **60** 701
[17] Nagashima Y, Morinaka Y, Kurihara T, Nagai Y, Hyodo T, Shidara T and Nakahara K 1998 *Phys. Rev.* B **58** 12676
[18] Cassidy D B, Hisakado T H, Tom H W K and Mills A P 2011 *Phys. Rev. Lett.* **107** 033401
[19] Cassidy D B, Hisakado T H, Tom H W K and Mills A P 2011 *Phys. Rev. Lett.* **106** 133401
[20] Cassidy D B, Hisakado T H, Tom H W K and Mills A P 2011 *Phys. Rev.* B **84** 195312
[21] Kawasuso A, Maekawa M, Miyashita A, Wada K, Kaiwa T and Nagashima Y 2018 *Phys. Rev.* B **97** 245303
[22] Kawasuso A, Wada K, Miyashita A, Maekawa M, Iwamori H, Iida S and Nagashima Y 2021 *J. Phys.: Condens. Matter* **33** 035006
[23] Wada K *et al* 2012 *Eur. Phys. J.* D **66** 37
[24] Terabe H *et al* 2015 *Surf. Sci.* **641** 68
[25] Gonze X *et al* 2002 *Comput. Mater. Sci.* **25** 478
[26] Blöchl P E 1994 *Phys. Rev.* B **50** 17953

[27] Perdew J P, Burke K and Ernzerhof M 1996 *Phys. Rev. Lett.* **77** 3865
[28] Barbiellini B, Puska M J, Torsti T and Nieminen R M 1995 *Phys. Rev.* B **51** 7341
[29] Nieminen R M and Puska M J 1983 *Phys. Rev. Lett.* **50** 281
[30] Hagiwara S, Hu C and Watanabe K 2015 *Phys. Rev.* B **91** 115409
[31] Callewaert V *et al* 2016 *Phys. Rev.* B **94** 115411
[32] Fazleev N G, Fry J L and Weiss A H 2004 *Phys. Rev.* B **70** 165309
[33] Jørgensen L V and Schut H 2008 *Appl. Surf. Sci.* **255** 231
[34] Suzuki R *et al* 1998 *Japan. J. Appl. Phys.* **37** 4636
[35] Böer K W 1990 *Survey of Semiconductor Physics* (Princeton, NJ: Van Nostrand-Reinhold)